# Retinex Computation: A Network Model

Jayanta Mukherjee R.Parthasarathi S.Goyal

Department of Computer Science & Engineering,
Indian Institute of Technology
Kharagpur, INDIA 721302

## Abstract

*In this work we propose a network model for the retinex computation. This model provides a better insight on the retinex theory. By drawing analogy from neuro-physiological activities in human vision system, we have suggested to replace the logarithmic function used in earlier models by a sigmoidal function. It has produced good color rendition. In addition in this case we do not require any color restoration filtering as a post-processing stage. Considering the interactions between rod and cone cells through the bipolar cells in the human vision system, we have further proposed the retinex computation using the diffusion of luminance component only. We found that this has produced almost similar color constancy and color rendition in the processed images.*

## 1 Introduction

In recent years a lot of interest has been shown in using the retinex theory for color enhancement and for obtaining color constancy. Edwin H. Land used the term retinex for the first time in the context of the processing of fluxes to generate lightness, which according to him could occur either in the retina or in the cerebral cortex or partially in both [1]. Since the location of that mechanism was uncertain it was termed as retinex in short. In the last paper on the retinex theory Land [2] had proposed a center/surround response model for spatially opponent colors in relation to the neuro-physiological functions of the individual neurons in the primate retina, lateral geniculate nuclei and cerebral cortex. This has lead to the development of an elegant computational model for achieving color constancy under varied spatial and spectral illumination of a scene. Using this model Jobson, Rahaman and Woodell [3] has developed computation techniques for color enhancement. Initially they used Single Scale Retinex(SSR) for achieving color constancy. Later they used Multi Scale Retinex(MSR) [4] which provides superior results to those obtained by SSR. They have also performed a post-processing of the retinex computed images for obtaining good color rendition. This operation is termed by them as color restoration filtering (CRF). Even though Jobson et al. [4] have shown good color renditions over different set of color images, Barnard and Funt [5] have pointed out that they still suffer from perturbing colors in some cases.

There are other approaches also for exploiting retinex theory to achieve color constancy. Hurlbert [6] proposed a computation model using an artificial neural network. Moore et al [7] implemented the retinex model through the Very Large Scale Integration(VLSI) of resistive networks. Barnard and Funt [5] decoupled the computation of color constancy from dynamic range compression using a trained neural network capable of predicting chromaticity of the scene illuminant [8]. They have shown that their technique is able to remove the complement color bleeding effect and the unwanted bluish artifacts are restored to their desired colors.

In this paper we have considered a network model for the retinex computation. We have considered the same MSR computational model used by Jobson et al [4] and performed Gaussian smoothing of the spectral bands by solving standard isotropic heat diffusion equation [9] in 2D. The iterative diffusion of spectral bands provides a network model for retinex computation. This model provides a better insight on the functioning of different computation blocks and computation stages. By drawing analogy from neurophysiological activities in human vision system, we have suggested to replace the logarithmic function by a sigmoidal function, a popular choice for simulating nonlinear behavior of artificial neurons in neural computation. We have further noticed the interaction between rod and cone cells through the bipolar cells [10] in the human vision system. As rods are responsible for achromatic vision and cones are responsible for chromatic vision we have proposed the retinex computation using the diffusion of luminance component. This has increased the speed of the computation. At the same time, this has delivered almost similar color constancy and color rendition in the processed images. In the following section we have described the multi scale retinex computation as used by Jobson et al [4]. Subsequently we present our network model and related modifications for retinex computation.

## 2 Traditional Multi-scale Retinex Computation

Consider a color image having pixel values in three spectral bands. Let us denote each spectral band as $I_i, i = 1, 2, 3$. The pixel value for the $i$th spectral band at $(x, y)$ location is denoted as $I_i(x, y)$. The single scale retinex is given by the following expression [3]:

$$R_i(x, y) = log(I_i(x, y)) - log(G(x, y) * I_i(x, y)) \quad (1)$$

where $R_i(x, y)$ is the retinex output for the $i$th spectral band at the $(x, y)$ pixel location in the image space. It may be noted that '$*$' denotes the convolution operation in the above expression. G(x,y) is the surround function which is a 2D Gaussian mask with the standard deviation $\sigma$ (uniform in both the principal directions). The MSR output is then given by the weighted sum of the outputs of the several different SSR outputs using Gaussian masks of different values of $\sigma$. Jobson et al [4] have used three surround functions and given equal weight-age for each of them for the retinex computation. Typically the values of $\sigma$'s taken by them are 15 ,80 and 250.

As MSR computation produced a greyish appearance of the processed images, Jobson et al [4] have used a color restoration function(CRF) as a post-processing of the retinex computation. The modified MSR is obtained as:

$$R'_i(x, y) = C_i(x, y).R_i(x, y) \quad (2)$$

Here $C_i(x, y)$ represents the color restoration function of the $i$th spectral band which is based on computation of the chromaticity coordinates. $C_i(x, y)$ is computed as:

$$C_i(x, y) = \beta.(log(\alpha.I_i(x, y)) - log(\Sigma_{i=1}^{S} I_i(x, y))) \quad (3)$$

where $\beta$ is the gain constant and $\alpha$ controls the strength of the nonlinearity and $S$ represents the number of spectral channels which is 3 for RGB color space. Using the color restoration function the final version of the multi-scale retinex is given by the following equation:

$$R''_i(x, y) = g.(R'_i(x, y) + b) \quad (4)$$

where $g$ is the final gain and $b$ is the offset value. The constants $g$ and $b$ intrinsically depend upon the implementation of the algorithm in the software. These are used to bring the values in the display domain. [1]

However we have observed that in our implementation the final retinex values ($R''_i$) have a very large dynamic range (typically, -32000 to 72000), which is image dependent also. We have used the full dynamic range to map the values in the range of 0 to 255 to get the display of the processed images. A typical pair of MSR processed images are shown in Figures 1 and 2.

Figure 1: (a) Original image: MOUNTAIN

One may observe the color bleeding effect in the second example (cf. Figure 2(b)). It may be noted here that we are not able to attain same visual quality as demonstrated by Jobson et al in [4]. This may be due

[1] On an enquiry to Dr. D. J. Jobson, it has been found that, at the immediate post-retinex stage an intermediate gain/ offset was applied as:
$R'(x, y) = R(x, y) * 28.44 + 128$.
Then color restoration was applied to yield $R''(x, y)$. Finally a final gain/offset was applied as:
$R'''(x, y) = (R''(x, y) - 20.) * 2.7$ to reach $0 - 255$ display.

Figure 1: (b) Retinex image by JRWMSRCR

Figure 2: (a) Original image: SUNSET

Figure 2: (b) Retinex image by JRWMSRCR

to the largely varying dynamic ranges obtained at the end of the computation, which are left untreated here. There was no mentioning of such a post-processing in [4]. But we feel that the major reason for the poor performance in our implementation is the improper selection of parameter values. As it is found to be extremely difficult to empirically choose these values due to the large dimensionality of the parameter space and the large computation overhead, the values of those parameters are taken from [4] and also from Dr. D. J. Jobson on electronic mail correspondences. However, this shows that their technique is heavily dependent on the proper tuning of the parameter values for getting the desired color rendition. The similar difficulties are also reported by Barnard and Funt [5].

## 3 Isotropic Diffusion and Network Model for MSR Computation

An image is convolved with a Gaussian mask (space surrounding function $G(x, y)$ in MSR computation) when it is fed as an initial input to the solution of the 2D heat diffusion equation. For a spectral band $I_i$ this may be written as:

$$\frac{\partial I_i}{\partial t} = w.(\frac{\partial^2 I_i}{\partial x^2} + \frac{\partial^2 I_i}{\partial y^2}), \text{where } w \text{ is a constant} \quad (5)$$

The well known discrete formulation of this equation is given below:

$$\begin{aligned} I_i^{(t+1)}(x, y) \quad = \quad & I_i^{(t)}(x, y) + w.(I_i^{(t)}(x-1, y) \\ & +I_i^{(t)}(x+1, y) + I_i^{(t)}(x, y-1) \\ & +I_i^{(t)}(x, y+1) - 4 * I_i^{(t)}(x, y)) \end{aligned} \quad (6)$$

The above equation shows that as the number of iterations increases the amount of smoothing will increase. In fact at the $n$th iteration, the resulting image is same as the convolved one with a Gaussian mask of an equivalent $\sigma$ of $\sqrt{2.n}$. It may also be noted that for the convergence of the above equation the value of $w$ should lie in between 0 and 0.25 [9]. Typically at $w = 0.25$ the equation assumes the following simple form:

$$\begin{aligned} I_i^{(t+1)}(x, y) \quad = \quad & \tfrac{1}{4}(I_i^{(t)}(x-1, y) + I_i^{(t)}(x+1, y) \\ & +I_i^{(t)}(x, y-1) + I_i^{(t)}(x, y+1)) \end{aligned} \quad (7)$$

Given these formulations one is capable of continuously varying the $\sigma$ of the surrounding function in MSR and accumulate the resulting retinex values after each iteration of the diffusion process. The operation at a single pixel is described by the network model given in Figure 3.

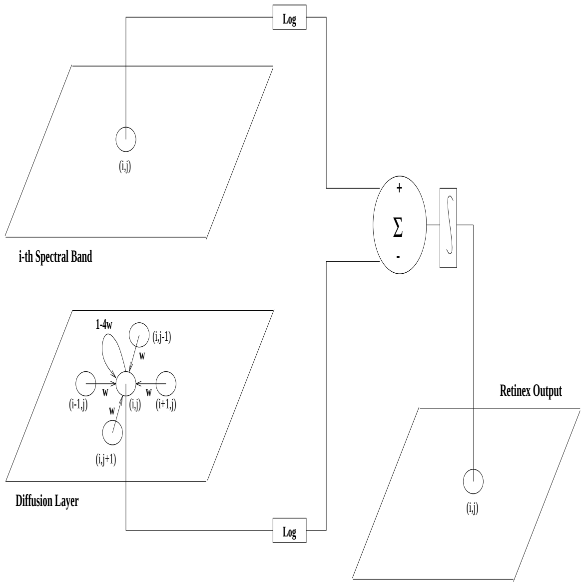


Figure 3. Network Model for MSR Computation

The mathematical expression for the MSR for the $i$th spectral band is given below:

$$R_i(x,y) = \frac{1}{N}.\Sigma_{t=1}^{N}(log(I_i^{(0)}(x,y)) - log(I_i^{(t)}(x,y))) \tag{8}$$

In the above equation $N$ is the total number of iteration and $I_i^{(0)}(x,y)$ is the original pixel value of the $i$th spectral band at $(x,y)$ pixel location. However as we find that it is not necessary to consider each and every iteration for accumulating retinex values, we have accumulated these values after a fixed interval (typically, 50 iterations in our implementation). The average of the accumulated values provide $R_i$ for each spectral band. We have obtained similar results as obtained previously [4] by applying similar color restoration operations with a different set of values for the respective parameters. In our case we have kept the value of $N$ as 10000. For lower values of N, the processed image appear more greyish and less bright. However, we have noticed that even if we increase the number of iteration to a great extent (say N=30000), the results do not improve much.

## 4 Replacement of Logarithmic Function by Sigmoidal Function

It is not clear how the retinex information is processed in our vision system. Land [1] has hypothesized that the retinex computation is carried out in the regions of the cerebral cortex. A type of elements called *blobs* are identified as responsible for this computation. However we have noticed from the network model that there are three stages of this retinex computation:

1. The diffusion layer where the smoothing or averaging of pixel values from surrounding space takes place and produces an inhibitory signal in proportion to the logarithm of the averaged value.
2. The excitation part on the other hand is contributed by the logarithm of the input pixel value.
3. Integration or accumulation of the single scale retinex values.

We propose that these computations are carried out by the bipolar cells in cooperation with the horizontal cells. The bipolar cells have a center/surround excitation/inhibition Receptive Field(RF) and this may be conjectured that the basic retinex computation (as given by the equation 1) is being carried out by those cells, whereas the diffusion process is carried out by the horizontal cells. It may be noted that all the cells in the visual path from rods and cones to ganglions give a graded response for an input excitation or inhibition [10]. In fact sigmoidal functions are being used for simulating the non-linear response behavior of artificial neurons. Hence we also propose here to replace the logarithmic function by a sigmoidal function, which takes the following form:

$$Sigmoid(x) = \frac{1}{(1+e^{(-(x+\theta)/T)})} \tag{9}$$

Here the parameters $\theta$ and $T$ denote the threshold and the scale for setting up of the activation level of the sigmoid function. The value of the threshold is taken as 128 where as scale has been fixed at 100 in our computation. So the modified retinex computational model is given below:

$$\begin{aligned} R_i(x,y) \quad = \quad & \tfrac{1}{N}.\Sigma_{t=1}^{N}(Sigmoid(I_i^{(0)}(x,y)) - \\ & Sigmoid(I_i^{(t)}(x,y))) \end{aligned} \tag{10}$$

### 4.1 Merits of using sigmoidal function

There are several reasons why someone should opt for a logarithmic function in computing retinex values. The logarithmic function is well known for their ability to bring large dynamic ranges to smaller ranges. The other reason for using the logarithmic function is that it decouples the illumination component from the reflectance in the retinex computation. The subtraction causes the removal of illumination component and retains the relative reflectance at the image point. Use of logarithmic function may be motivated also by the fact that rods and cones in our retina respond logarithmically to the optical illumination [10].

However the sigmoidal function has its advantages too. It is defined for the whole real axis, whereas logarithm is defined for only positive values. Specially, one has to take care of handling zeroes in this case. The dynamic range of the output of the logarithmic function is from $-\infty$ to $+\infty$. The output of a sigmoidal function has the dynamic range from 0 to 1. In fact one of the difficulty in the retinex computation is the suitable mapping of final retinex values to the displayable range (typically 0 to 255). The use of logarithmic function in this case causes a wide variation of dynamic ranges for different types of images. The sigmoidal function on the other hand produces a dynamic range within $-1$ to 1 (cf. equation ( 10)). It is interesting to note that in a recent paper [11] sigmoidal functions are used for displaying high contrast images. The property of dynamic range compression of sigmoidal functions facilitates these operations.

### 4.2 Color restoration

We have observed that the use of sigmoidal functions in the retinex computation directly provides the required color rendition in the processed images. Hence there is no need of color restoration operation in the post-processing of retinex computed images. Moreover as the dynamic ranges are restricted within a known interval, we have conveniently applied histogram stretching here. In this case, range of values containing 98% of the pixels are used for mapping to the displayable range. In Figures 4(a) & (b) images obtained from MSR computation using sigmoid functions are shown. One may note that the color bleeding phenomenon as observed earlier (cf. Figure 2(b) ) does not appear in this case (cf. Figure 4(b)).

Figure 4(a) Using sigmoidal function : for MOUNTAIN

Figure 4(b) Using sigmoidal function: for SUNSET

## 5 Rod-Cone Interaction and Retinex Computation

So far in all the available retinex computational model [2] [3] [4] [5] , the information processing is solely restricted to an individual spectral band. But in the visual path of our vision system, interactions between rods and cones also take place in bipolar cells. In fact there are bipolar cells where four rods and a single cone are connected [12]. This connectivity has encouraged us to consider the diffusion of the luminance values only (as rods are responsible for luminance encoding). Then the retinex values for individual spectral band is computed with respect to these diffused luminance values. Given a color image in the RGB space, in this work the luminance value $L$ is computed at any pixel using the following equation:

$$L(x,y) = 0.177r(x,y) + 0.813g(x,y) + 0.011b(x,y) \tag{11}$$

where $r(x,y)$, $g(x,y)$ and $b(x,y)$ are respectively red, green and blue components at the image point $(x,y)$.

Hence the diffusion of the luminance component of the image is expressed as:

$$\begin{aligned} L^{(t+1)}(x,y) \quad = \quad & \tfrac{1}{4}.(L^{(t)}(x-1,y) + L^{(t)}(x+1,y) \\ & +L^{(t)}(x,y-1) + L^{(t)}(x,y+1)) \end{aligned} \tag{12}$$

Finally, the retinex values computed using these diffused values are given below:

$$\begin{aligned} R_i(x,y) \quad = \quad & \tfrac{1}{N}.\Sigma_{t=1}^{N}(Sigmoid(I_i(x,y)) - \\ & Sigmoid(L^{(t)}(x,y))) \end{aligned} \tag{13}$$

In this case also we have not used any color restoration after obtaining the retinex values. It may also be noted that as we are carrying out the diffusion process only in one component (the luminance component), the algorithm runs much faster in this case (almost three times of the technique described in the previous section).

## 6 Results

We have experimented with various images for comparing the performances of our proposed algorithms. We have made our observations for the following three techniques:

1. MSR computation as proposed by Jobson et al. (JRW-MSRCR).

2. MSR computation using sigmoidal function (SIG-MSR).

3. MSR computation using luminance value in the diffusion process and sigmoid function in the retinex computation (LUM-SIG-MSR).

Here we present two typical results. One is with an image having wide range of variation (cf. Figure 5(a) of 'BRIDGE') and the other one is photographed with active (and artificial) illumination (cf. Figure 6(a) of 'CITY-PROFILE'). These are taken from the web-site at *http://dragon.larc.nasa.gov /viplab /projects /retinex /retinex.html*. It may be noted that the processed images by JRW-MSRCR are directly obtained from the same web-site. For each the retinex processed images using JRW-MSRCR, SIG-MSR and LUM-SIG-MSR are shown in Figures 5(b) to (d) and 6(b) to (d) respectively. The computational advantages in SIG-MSR and LUM-SIG-MSR techniques against JRW-MSRCR are in their speed and less number of parameters in adjusting the retinex values to the displayable range. LUM-SIG-MSR runs even faster (three times) than SIG-MSR method. Another advantage in these techniques is that they do not require any color restoration filtering (CRF) operation. Color bleeding effects are also not observed in these cases. On the other-hand, we found that JRW-MSRCR produces excellent color rendition in various images. Moreover LUM-SIG-MSR fails to deliver good quality of color rendition for artificially illuminated images. Our observations are summarised in the Table 1.

From the figures one may observe that the results obtained by JRW-MSRCR are excellent. It is interesting to note that for the image 'CITY PROFILE', SIG-MSR technique provides more detailed information (cf. Figure 6(c)). In some places it has recovered greenish spots and the small objects on the road are more highlighted in the processed images. It has been also noted that LUM-SIG-MSR performs poorly in the artificially illuminated scene (cf. Figure 6(d)).

Figure 5(a) BRIDGE: original

Figure 5(b) BRIDGE: JRWMSRCR

Figure 5(c) BRIDGE: SIGMSR


Figure 5(d) BRIDGE: LUM-SIG-MSR


Figure 6(a) CITY PROFILE: original


Figure 6(b) CITY PROFILE: JRWMSRCR


Figure 6(c) CITY PROFILE: SIGMSR


Figure 6(d) CITY PROFILE: LUM-SIG-MSR

Table 1: **Comparitive assesments of various algorithms**

| | JRW-MSRCR | SIG-MSR | LUM-SIG-MSR |
|---|---|---|---|
| 1. | Largely varying dynamic ranges. | Dynamic ranges are fixed within a known limit. | Dynamic ranges are fixed within a known limit. |
| 2. | Heavily dependent on parameter tuning. | More robust with less number of parameters. | More robust with less number of parameters. |
| 3. | CRF required. | CRF not required. | CRF not required. |
| 4. | Color bleeding effect observed. | No color bleeding effect. | No color bleeding effect. |
| 5. | Slow computaion speed. | Moderate computation speed. (Typically three times of JRW-MSRCR). | Fast computation speed. (Typically three times of SIG-MSR). |
| 6. | Delivers excellent visual quality in the most of the cases. | Delivers good quality. | Delivers good quality. Images appears greyish in artificial illumination. |

## 7 Conclusion

In this paper we have developed a network model for the retinex computation by performing Gaussian smoothing of the spectral bands through their isotropic diffusions in 2D space. This model provides a better insight on the functioning of different computation blocks and computation stages. In our model we have also suggested to replace the logarithmic function by a sigmoidal function, a popular choice for simulating nonlinear behavior of artificial neurons in neural computation. We have found that the use of sigmoidal functions also provides color constancy with good color rendition. In fact in this case we do not require any color restoration filtering in the post-processing stage. We have further studied the connections of different types of cells in the visual path of human vision system. We have noticed the interaction between rod and cone cells through the bipolar cells in the human vision system. As rods are responsible for achromatic vision and cones are responsible for chromatic vision we have proposed the retinex computation using the diffusion of luminance component. This has produced similar color constancy and color rendition in the most of the cases.

## Acknowledgement

The authors gratefully acknowledge the help received from Dr. D.J.Jobson for implementing their multi-scale retinex algorithm.

## References

[1] Edwin H. Land, "The retinex theory of color vision," *Scientific American*, vol. 237, no. 6, pp. 108 – 129, Dec. 1977.

[2] Edwin H. Land, "Recent advances in retinex theory.," *Vision Research*, vol. 26, pp. 7–21, 1986.

[3] Daniel J. Jobson, Z.Rahman, and Glenn A. Woodell, "Properties and performance of a center/surround retinex," *IEEE Transactions on Image Processing*, vol. 6, no. 3, pp. 451 – 462, March 1997.

[4] Daniel J. Jobson, Z.Rahman, and Glenn A. Woodell, "A multiscale retinex for bridging the gap between color images and the human observation of scenes," *IEEE Transactions on Image Processing: Special Issue on Color Processing*, vol. 6, no. 7, pp. 965 – 976, July 1997.

[5] Kobus Barnard and Brian Funt, "Investigations into multi-scale retinex," *Colour Imaging in Multimedia '98, Derby, UK*, pp. 9–17, March 1998.

[6] A. C. Hurlbert, "Formal connections between lightness algorithms," *Journal of the Optical Society of America A*, vol. 3, no. 10, pp. 1684 – 1693, Oct. 1986.

[7] Andrew Moore, John Allman, and Rodney M. Goodman, "A real-time neural system for color constancy," *IEEE Transaction on Neural Networks*, vol. 2, no. 2, pp. 237 – 247, Mar. 1991.

[8] Brian V. Funt, Vlad Cardei, and Kobus Barnard, "Neural network color constancy and specularly reflecting surfaces," *Proceedings, AIC Color 97 Kyoto 8th Congress of the International Color Association, Japan*, May 25-30 1997.

[9] Harry Wechsler, *Computational Vision*, Academic Press, Inc., 1990.

[10] A.C.Guyton and J.E. Hall, *Textbook of Medical Physiology*, W.B. Saunders Company, ninth edition, 1996.

[11] J. Tumblin, J. K. Hodgins, and B.K. Guenter, "Two methods for display of high contrast images," *ACM Transactions on Graphics*, vol. 18, no. 1, pp. 56–94, January, 1999.

[12] C.C.Chatterjee, *Human Physiology*, vol. II, Medical Allied Agency (India), Calcutta, ninth edition, 1983.